

Forward-Facing Steps Induced Transition in a Subsonic Boundary Layer

Hui Zhu* and Song Fu*

*School of Aerospace Engineering, Tsinghua University, Beijing 100084, China

Abstract

A forward-facing step (FFS) immersed in a subsonic boundary layer is studied through a high-order Flux Reconstruction (FR) method to highlight the flow transition induced by the step. The step height is a third of the local boundary-layer thickness. The Reynolds number based on the step height is 720. Inlet disturbances are introduced giving rise to streamwise vortices upstream of the step. It is observed that these small-scale streamwise structures interact with the step and hairpin vortices are quickly developed after the step leading to flow transition in the boundary layer.

1. Introduction

The flow phenomenon of transition from laminar to turbulent flow has long attracted the attention of researchers. On one hand, it is one of the problems that is not totally solved in classic Newtonian mechanics, while on the other hand, it is commonly observed in the engineering fields as well. However, the intrinsic nonlinearity of the Navier-Stokes equation adds to the difficulty of understanding the transition phenomena.

The nonlinearity property also gives rise to some complicated flow physics. For example, for two-dimensional geometries such as Forward-Facing Steps (FFS) and Backward-Facing Steps (BFS), an inflow condition with disturbance may induce three-dimensional flow structures, which is a key step in transition from laminar to turbulent flows.

Although similar in geometry configuration, BFS has accumulated much more detailed research results than FFS. For instance, De Brederode and Bradshaw [1] studied the separation region of BFS experimentally, and Eaton and Johnston [2] reviewed the reattachment in the downstream of BFS. Nevertheless, there is much less research on FFS. Chiba et. al. [3] made experiments on flow through a forward-facing step channel of both Newtonian and non-Newtonian fluid. Largeau and Moriniere [4] measured wall pressure fluctuations and flow fields in separated flows over a forward facing step. Camussi et. al. [5] analyzed statistical properties of wall pressure fluctuations over a forward facing step. Stürer, Gyr and Kinzelbach [6] and Zukoski [7] studied low speed laminar separation flow and supersonic turbulent separation flow over a forward facing step respectively.

The papers referred above mainly falls into two Reynolds number ranges. One is the low-Reynolds-number case, such that the inlet flow is laminar, and the evolution of small disturbances is analyzed. The other is the high-Reynolds-number case, where the upstream flow is fully turbulent, and the basic focus is pressure distributions and flow regime. However, few researches have been published for the Reynolds number in between, which is called the mid-Reynolds-number case here. In this range, the inlet flow is laminar, yet the FFS may induce flow transition. Moreover, most of the papers referred above pay their attention to forward-facing steps in channel flows, while the FFS in the boundary layer flow is more or less neglected.

The thesis of Edelmann [8] focused on the transitional effects of the FFS in boundary layers. A blowing-suction pulse disturbance is set on the wall upstream of the FFS, and the evolution of this wave package is studied. Numerous flow cases are considered, including a Mach number range from 0.15 to 1.06, Reynolds number based on the step height from 400 to 4440, and zero-or-favorable streamwise pressure gradient condition. Results were obtained by linearized flow instability analysis, and direct numerical simulation of the disturbance Navier-Stokes equation.

It is well known that there are two types of transition in boundary layer flows, that is, natural transition and bypass transition. In a natural transition, the inflow disturbances, typically the Tollmien-Schlichting waves, experience an exponential growth in the first stage, then the nonlinearity brings up disturbance in different wavelengths, and finally the vortices break down, where the flow becomes fully turbulent. By contrast, the linear stage does not exist in the bypass transition. Due to the larger amplitude of inflow disturbance, or other kinds of disturbances such as obstacles on walls and fluctuations from outside of the boundary layer, the transitional flow skipped the linear growth stage, and non-linear instability is triggered directly.

Previous studies have demonstrated that three-dimensional obstacles in boundary layers could trigger flow transition for flows at a certain Reynolds number range. For example, diamond-shaped or cylinder-shaped obstacles in boundary layers can bring up three-dimensional horse-shoe vortices, and lead the boundary layer to become fully turbulent.[9] However, how a two-dimensional obstacle, such as the FFS, could affect the transitional boundary layer is not so clear yet. The key difference here is that, three-dimensional horse-shoe vortices which plays a key role in obstacle flows does not exist in the FFS flow, therefore the mechanism in boundary-layer transition should be distinct.

This paper presents a numerical study of the influence of FFS on the transition of boundary-layer flows, based on the high-order Flux Reconstruction (FR) method with the Implicit Large Eddy Simulation approach (ILES). In Section 2, a brief introduction of the numerical methods is given. Then in Section 3, the cases are described, and the flow physics are studied in detail. Finally the conclusions are drawn in Section 4.

2. Numerical Methods

Transitional flows are governed by compressible Navier-Stokes equations. In Cartesian coordinates, the Navier-Stokes equations can be written as:

$$\frac{\partial \mathbf{U}}{\partial t} + \sum_{i=1}^3 \frac{\partial \mathbf{F}_i}{\partial x_i} - \sum_{i=1}^3 \frac{\partial \mathbf{F}_i^v}{\partial x_i} = \mathbf{0} \quad (1)$$

where

$$\mathbf{U} = \begin{bmatrix} \rho \\ \rho u_j \\ \rho E \end{bmatrix}, \quad \mathbf{F}_i = \begin{bmatrix} \rho u_i \\ \rho u_i u_j + p \delta_{ij} \\ \rho u_i H \end{bmatrix}, \quad \mathbf{F}_i^v = \begin{bmatrix} 0 \\ \sigma_{ij} \\ \sum_{k=1}^3 \sigma_{ik} u_k - q_i \end{bmatrix}, \quad j = 1, 2, 3 \quad (2)$$

Here, \mathbf{U} is the conservative variables, \mathbf{F} and \mathbf{F}^v are convective and viscous fluxes respectively, and ρ , p and u are density, pressure and velocity components. For perfect gas, E is specific total energy, $E = e + \rho u^2 / 2$, and e is specific internal energy, $e = RT / (\gamma - 1)$. H is specific total enthalpy, $H = E + p / \rho$, where R is the gas constant, and γ is the specific heat ratio. σ_{ij} and q_i are components of viscous stress tensor and heat conduction vector respectively.

Transitional flows are dominated by waves and vortices of different sizes. Thus, a numerical method that can resolve a wide range of length scales is required. Among traditional CFD methods, the Finite Difference Method (FDM) is usually applied to such flows, due to its high resolution ability. However, boundary conditions and parallel computing are not easy to treat in FDM, since the scheme is not compact typically.

On the other hand, the resolution ability of high-order Finite Element Methods (FEM), such as Flux Reconstruction (FR) and Discontinuous Galerkin (DG), is similar to that of FDM, meanwhile the numerical scheme involves only immediate neighboring cells. Therefore, it is much easier to apply boundary conditions in high-order FEM. In transitional flows, both solid wall and outflow boundaries could play important roles in numerical simulations, thus the advantage of high-order FEM is not trivial.

In this paper, an in-house CFD solver called MULTiphysics SIMulation Code (MUSIC) is adopted to calculate the transitional flows induced by forward-facing steps. MUSIC is a high-order Flux Reconstruction solver on unstructured meshes. Here a brief introduction of the numerical method is demonstrated.

2.1 Basic Ideas of the Flux Reconstruction Method

The Flux Reconstruction method was first introduced by Huynh in hexahedral cells [10], and later Wang [11] developed this method to other kinds of cells including simplexes. The FR method can be categorized into discontinuous finite element methods. It involves multiple degrees of freedom (DOFs) in one computation cell, just like standard FEM, and uses Riemann solvers to calculate fluxes on cell interfaces, which resembles Finite Volume Method (FVM).

The DOFs in cells are variables at certain points called Solution Points (SP), and flux between cells are evaluated at points on cell interfaces called Flux Points (FP). In order to achieve the best numerical accuracy, Gauss quadrature points are chosen as SPs and FPs.

The first step of the FR method is to reconstruct a polynomial of flux in a cell based on variables at SPs. This polynomial is discontinuous at cell interfaces, thus not applicable directly. Nevertheless, a Riemann solver can be employed to get a common flux at FPs, and a correction to the flux polynomial is added. Then, the derivative of the corrected polynomial is used to propagate the solution to the next time step.

These two steps are known as the reconstruction step and the correction step respectively. Therefore, the Flux Reconstruction method is called Correction Procedure via Reconstruction (CPR) as well.

2.2 Calculation of the Viscous Term

The procedure described above is only available for the first-order convection term, and the second-order viscous term should be calculated in a different way. Here, an additional set of equations is introduced to evaluate the gradient of conservative variables:

$$\mathbf{R} = \nabla \mathbf{U} \quad (3)$$

This augmented equation is also a first-order partial differential equation (PDE), and can also be solved by the FR method, although the computational cost may be high. Bassi and Rebay [12] developed a simple algebraic scheme called BR2 to achieve the solution approximately, and Huynh [13] introduced this scheme to the FR method. The BR2 scheme is a compact one involving only the immediate neighboring cell, and also purely symmetric, which mimics the elliptic property of the viscous term.

2.3 Time Integration

Since an Implicit Large Eddy Simulation (ILES) approach is to be used, the calculation has to take the unsteady effect into account. For the high-order Flux Reconstruction method, explicit Runge-Kutta time integration could be an appropriate choice, because it finds a balance between precision and efficiency. Here, a Strong Stability Preserving (SSP) third-order Runge-Kutta [14] scheme is adopted. The coefficients in the SSP Runge-Kutta scheme are carefully tuned to improve the numerical stability, and the maximum CFL number could reach 1.0. The scheme is as follows:

$$\begin{aligned} u^{(1)} &= u^n + \Delta t L(u^n, t^n) \\ u^{(2)} &= \frac{3}{4}u^n + \frac{1}{4}u^{(1)} + \frac{1}{4}\Delta t L(u^{(1)}, t^n + \Delta t) \\ u^{n+1} &= \frac{1}{3}u^n + \frac{2}{3}u^{(2)} + \frac{2}{3}\Delta t L\left(u^{(2)}, t^n + \frac{1}{2}\Delta t\right) \end{aligned} \quad (4)$$

2.4 Characteristic Outflow Boundary Condition

The outflow boundary condition plays an important role in the calculation. If treated improperly, spurious flow structures may come up in the vicinity of the outflow boundary, thus deteriorate the results.

The Flux Reconstruction method applies the boundary condition at boundary Flux Points, using Riemann solver for inviscid flux and Bassi-Rebay 2 scheme mentioned in 2.2 for viscous flux respectively. Comparing to the Finite Volume Method, virtual mesh is not necessary herein.

In this paper, the flows are all at low Mach number, so that the outflow condition is always subsonic. Only one outflow parameter should be fixed, according to the one-dimensional Riemann invariant theory. Here the back pressure is given, while all other values are extrapolated from the flow. This procedure is able to minimize the fake disturbance caused by the outflow condition.

2.5 Implicit Large Eddy Simulation

There has been a heated discussion on whether Large Eddy Simulations (LES) can be applied to transitional flows. Some researchers infer that the resolving ability of LES helps to capture the waves in the transitional phase, while others insist that the sub-grid scale is incorrectly modelled by the standard Smagorinsky model. Both sides have their points, whereas the resolving part should play a more important role, since structures in large scale dominates the flow until late transitional phase, and the sub-grid scale (SGS) model should not interfere the flow too much.

In this paper, an implicit Large Eddy Simulation approach based on the high-order Flux Reconstruction method is adopted. The high-order FR method can well capture flow structures on a relatively coarse mesh, and the implicit LES approach minimizes the SGS effect. This method finds a balance between the two viewpoints mentioned here.

3. Results and Discussion

3.1 Case Description

The transitional flow over an FFS inside a subsonic flat plate boundary layer is simulated. Due to limited computer resources, the streamwise length computed is only 100 times of the height of the FFS, denoted as h in the following. The step is set at the streamwise location of $x = 0$. The inlet plane is set at 50 times of h upstream of the FFS, while the outflow plane is located at 50 times of h downstream of the step. The upper boundary is set as farfield boundary condition at 50 times of h , thus minimizes its effect on the boundary layer. The characteristic outflow boundary described in Section 2.4 is applied at the outflow boundary.

The Reynolds number based on the height of FFS is 720, and the streamwise Reynolds number is 330624, which stays in the middle of transition stage from laminar to turbulent flows, according to the classic boundary layer theory. The height of FFS is one-third of the thickness of boundary layer at inlet plane, and the spanwise range is 30 times of h . At the inlet plane, the Reynolds number based on the streamwise location from the leading edge of the flat plate is 186624, meaning that the transition procedure is beyond the linear growth phase. Therefore, a disturbance with a finite amplitude is superimposed to the Blasius velocity profile. The final inlet velocity profile is as follows:

$$u = u_{Blasius} \times (1 + \alpha_1 \sin(\pi y / \delta) * \cos \omega t) \times (1 + \alpha_2 \cos(\beta \pi z / L)) \quad (5)$$

where α_1 and α_2 is the amplitude of the disturbance, which is both set as 0.05 here, and δ, L are the thickness of boundary layer and the spanwise width respectively. The disturbance is periodic in time with a frequency of ω , in order to better simulate real inlet flow.

The inlet velocity profile is illustrated in Figure 1. Due to the property of sine and cosine functions, the mean profile is identical to the Blasius solution, and the maximum and minimum curves are perturbed velocity profiles with the maximum magnitude. This disturbance is chosen to be nearly neutral in the flat plate boundary layer, which does not grow or decay in the streamwise direction, as is discussed in the following sections.

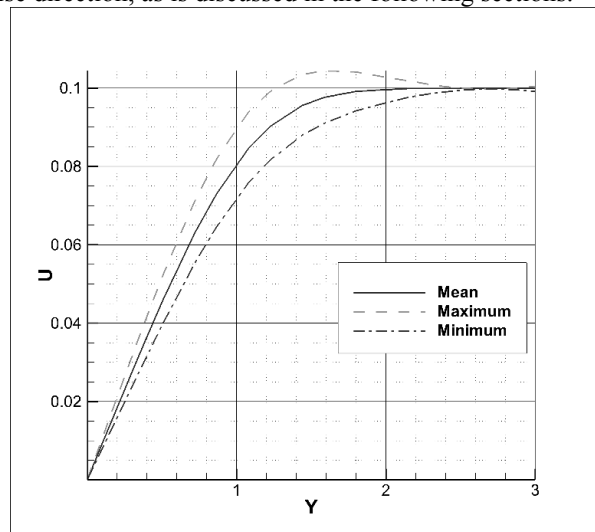


Figure 1: Velocity Profile at the Inlet Plane

3.2 Mean Flow Analysis

Flat plate boundary layer flows serve as a basis for the study of transitional flows. Here, a flat plate with the same inlet flow condition and other configurations is calculated, in order to find whether such disturbance will trigger the flow transition itself.

Fig. 2 shows the averaged streamwise velocity profile at different streamwise locations of the flat plate boundary layer flow calculated. The flowfield is averaged both in time series and in the spanwise direction, with more than 60 million samples altogether. It is found that at all the streamwise planes shown in the figure, the velocity profiles resemble each other, with almost identical slope at the wall. This supports the viewpoint that the flow stays laminar in this case.

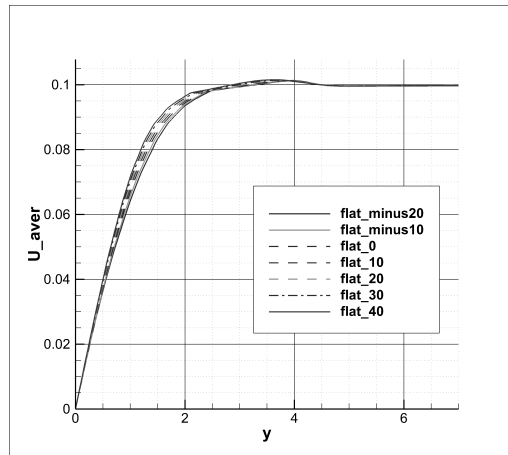


Figure 2: Averaged Streamwise Velocity Profile for the Flat Plate.

Non-dimensional turbulent intensity \sqrt{k}/U of the flat plate flow is shown in Fig. 3. Here k is the turbulent kinetic energy, and U is the magnitude of local velocity. This variable takes both averaged local velocity and turbulent effect into effect, eliminating the sharp velocity gradient in the boundary layer. For the flat plate flow, the value of non-dimensional turbulent intensity is no larger than 0.04 in the whole boundary layer, also indicating that the flow is not experiencing a transition. These figures above demonstrate that the disturbance added at the inlet plane could not trigger the boundary layer transition by itself.

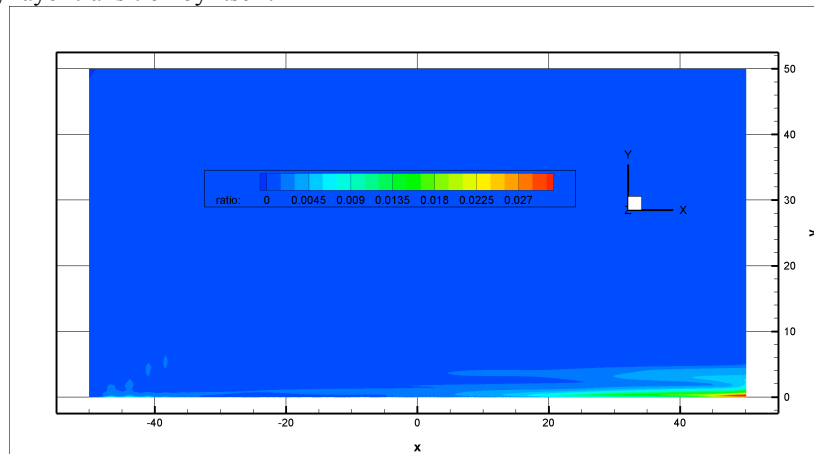


Figure 3: Non-Dimensional Turbulent Intensity of the Flat Plate.

On the other hand, with respect to the forward-facing step, the case is quite different. Figure 4 presents the time-averaged streamline and non-dimensional turbulent intensity in the vicinity of the step. Two separation regions can be observed: one at the upstream of the FFS, the other at the top of the step. In both regions, streamlines bears complicated topology, including multiple vortices and saddle points. It is noteworthy that the first reattachment point locates at the vertical wall of the step instead of the corner, which means that the two separation regions are isolated. Meanwhile, high non-dimensional turbulent intensity coincides in these two regions, indicating that these separations are possibly amplifying the inflow disturbance and triggering transition. On the other hand, the streamlines outside the separation regions become concave, which may be a source of flow instability according to classic theory as well.

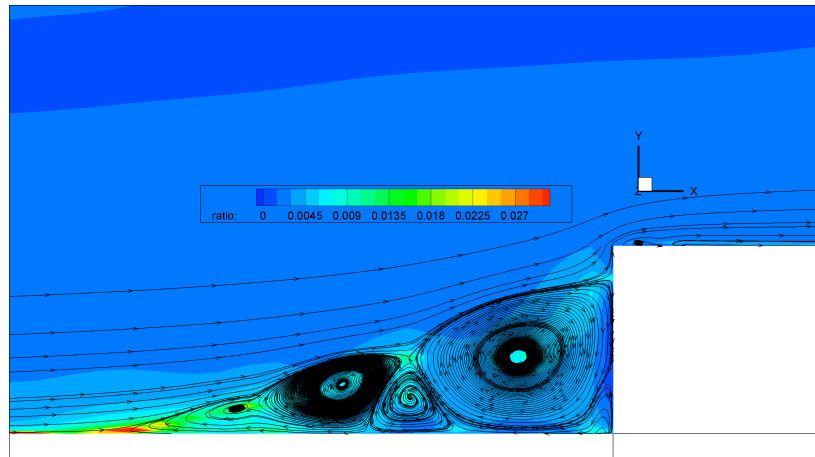


Figure 4: Streamlines of the mean flow at the vicinity of the Step

The time-averaged streamwise velocity profile is given in Figure 5. At the upstream of the step, due to the separation effect, slopes at the wall are significantly small, while at the downstream side, the velocity profiles are developing rapidly, with the slope at the wall growing. This is also an evidence of transitioning boundary layer.

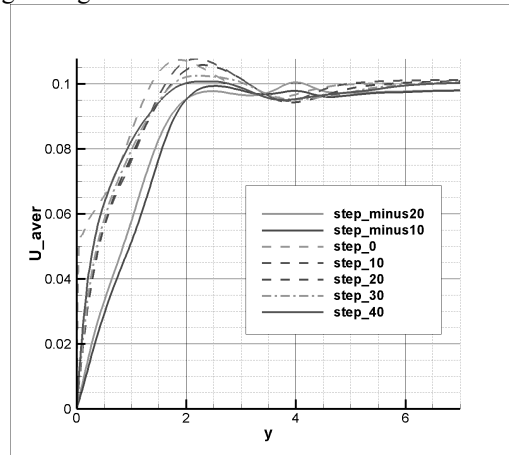


Figure 5: Averaged Streamwise Velocity Profile for the Forward-Facing Step

3.3 Instantaneous Flow Analysis

The instantaneous slices of streamwise velocity over the flat plate and the FFS is shown in Fig. 6. The snapshot time is at non-dimensional time $t = 3000$. For the flat plate, the inlet disturbance does not grow at the entire computation domain. On the other hand, the disturbance starts to grow at around $x = -20$ for the FFS case. Bell shaped structures appears in front of the step, and turns into complicated structures at the downstream of the step.

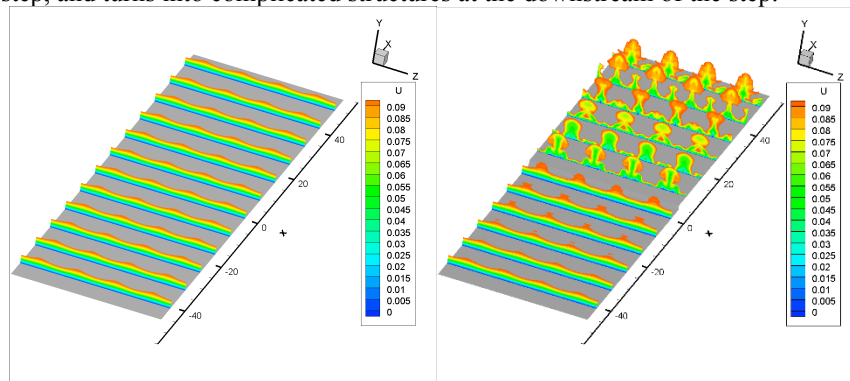
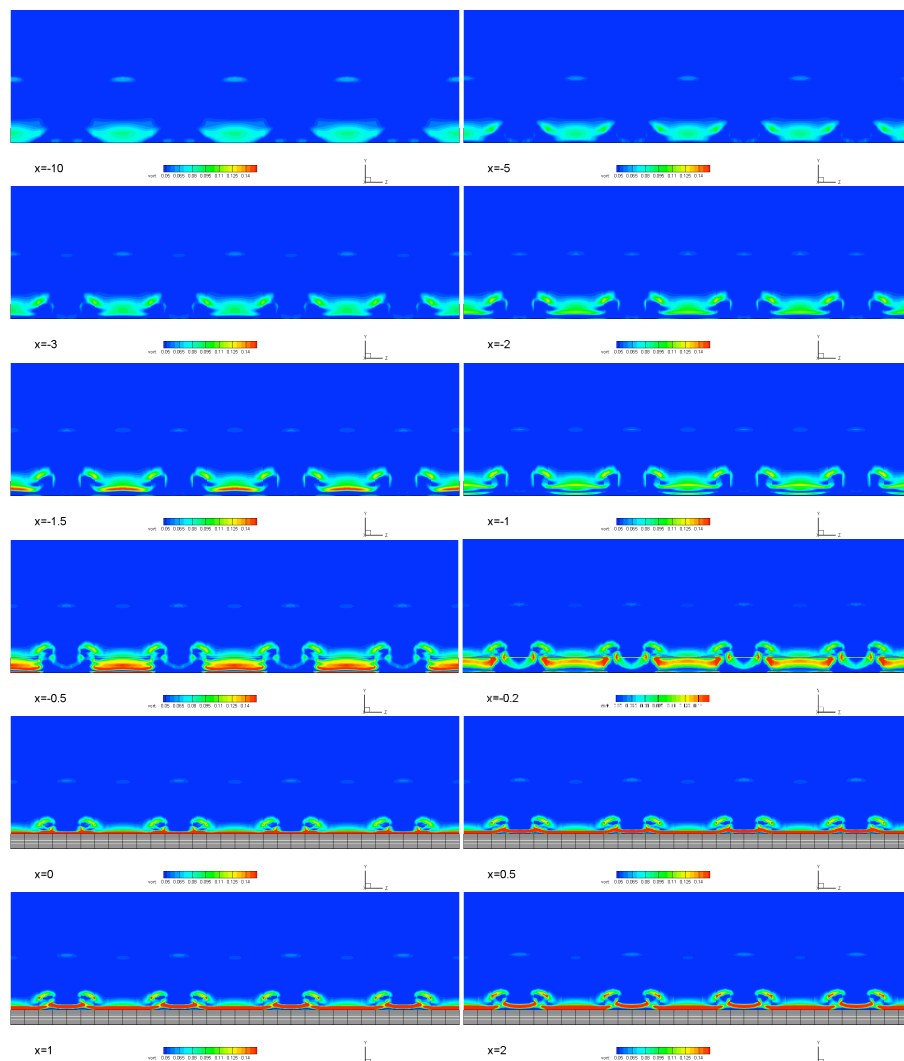


Figure 6: Instantaneous Slices of Streamwise Velocity. Left: Flat Plate. Right: Forward-Facing Step

Streamwise slices of instantaneous vorticities in the vicinity of the step is shown in Fig. 7. The snapshot time is at non-dimensional time $t = 2700$. The incoming disturbance behaves as weak vortices in the boundary layer. When it reaches $x = -10$, small scale secondary structures begin to emerge on the edge of these weak vortices, and continues to grow and move upwards in the first separation region. At $x = -0.5$, the main vortices become much stronger and gets lower, and the secondary vortices go further upwards and deform into pairs of vortices. Then at the corner plane where $x = 0$, the lower main vortices are blocked by the step, while the secondary vortices climb over the step and continue to grow stronger. At $x = 5$, these secondary vortices are still significant. It can be found that these secondary vortices lies in the streamwise direction, and continuous become stronger as it goes downstream. Meanwhile, the vertical location of these vortices is going upwards in the upstream of the step, but stays stationary later in the downstream of the step. This indicates that the structures observed here is actually a set of streamwise vortices, which resembles the experimental results of Stür [6].

To further investigate the effect of the forward-facing steps on boundary layer transition, instantaneous flow fields at upstream and downstream of the step are demonstrated in Figure 8 and Figure 9 respectively. Q-criterions colored by the streamwise velocity are used to show the vortex structures. The inlet disturbance experiences a decay at the first stage, and then at around $x = -25$, weak streamwise vortices are formed at the bottom of the boundary layer, according to Figure 12. Due to the blockage effect of the FFS, the vortices grow and hit the step wall, and small scale structures are formed, confirming the previous analysis of Fig. 7. Another set of weaker streamwise vortices form in the concave-streamline regions outside separation regions, and merge into the vortices mentioned above at the reattachment point of the second separation region. The small structures introduce a new set of spanwise vortices. Due to their small-scale sources, the spanwise vortices are high in frequency, which trigger secondary instabilities in the boundary layer. Further downstream, these vortices are raised and deform into classic hairpin vortices that is the key to later transition. It is observed that although all the structures mentioned above locates in the near-wall scope of the boundary layer, another set of hairpin vortices are induced as well, which locates in the outer region of the boundary layer. All the flow phenomenon mentioned above resembles the Klebanoff modes in the boundary layer instability problem.



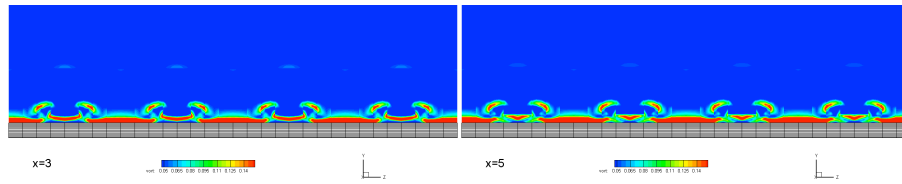


Figure 7: Instantaneous Slices of Vorticity of the Forward-Facing Step

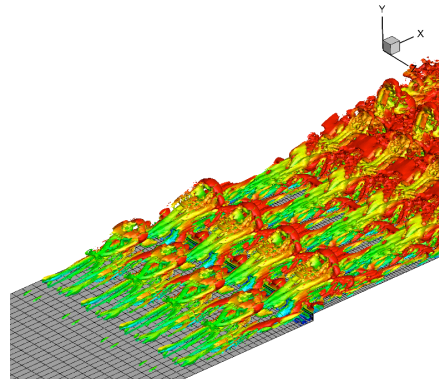


Figure 8: Instantaneous Isosurface of Q-Criterion at the Upstream of the Forward-Facing Step

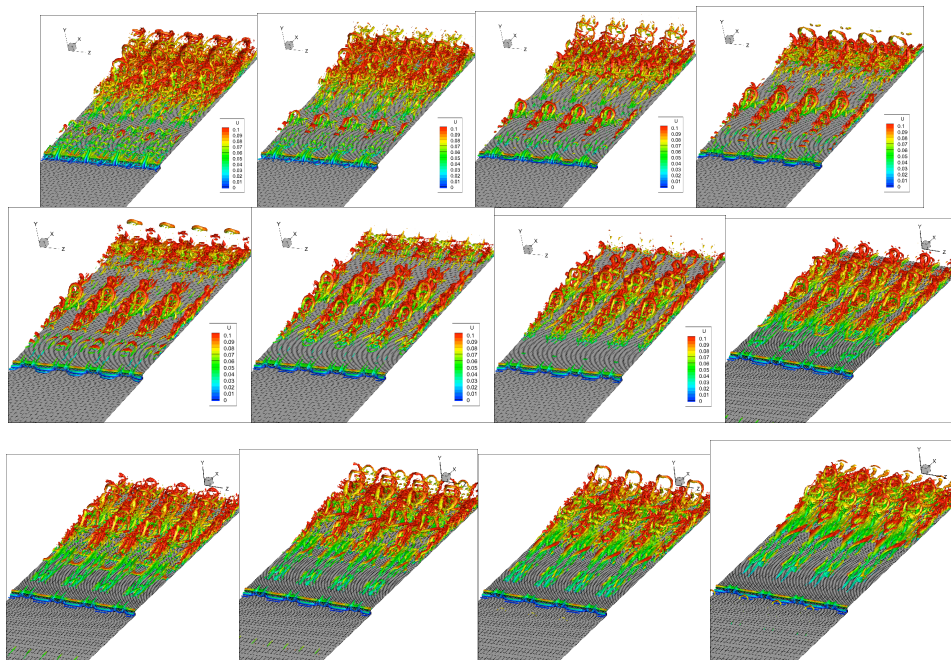


Figure 9: Instantaneous Isosurface of Q-Criterion at the Downstream of the Forward-Facing Step. Snapshot Time: 2400, 2450, 2500, 2550, 2600, 2650, 2700, 2750, 2800, 2850, 2900, 2950

References

- [1] De Brederode, V. 1975. Three-dimensional flow in nominally two-dimensional separation bubbles. I. Flow behind a rearward-facing step. PhD Thesis, Department of Aeronautics, Imperial College, London University.
- [2] Eaton J. K. and J. P. Johnston. 1981. A review of research on subsonic turbulent flow reattachment. *AIAA J.* 19: 1093-1100

-
- [3] Chiba, K., R. Ishida and K. Nakamura. 1995. Mechanism for entry flow instability through a forward-facing step channel. *J. Non-Newton Fluid* 57: 271-282
- [4] Largeau J. F. and V. Moriniere. 2007. Wall pressure fluctuations and topology in separated flows over a forward-facing step. *Exp. Fluids* 42: 21-40
- [5] Camussi, R., M. Felli, F. Pereira, G. Aloisio and A. Di Marco, Statistical properties of wall pressure fluctuations over a forward-facing step. *Phys. Fluids* 20: 075113
- [6] Stürer, H., A. Gyr and W. Kinzelbach. 1999. Laminar separation on a forward facing step. *Euro. J. Mech-B/Fluids* 18: 675-692
- [7] Zukoski, E. E. 1967. Turbulent boundary-layer separation in front of a forward-facing step. *AIAA J.* 5: 1746-1753.
- [8] Edelmann C. A. 2014. Influence of forward-facing steps on laminar-turbulent transition. PhD Thesis. Institute of Aerodynamics and Gas Dynamics, University of Stuttgart.
- [9] Duan, Z. W., Z. X. Xiao and S. Fu, 2014. Direct numerical simulation of hypersonic transition induced by an isolated cylindrical roughness element. *Sci. China-Phys. Mech. Astron.* 57: 2330-2345
- [10] Huyhn H. T. 2007. A flux reconstruction approach to high-order schemes including Discontinuous Galerkin methods. *AIAA paper* 2007-4079
- [11] Wang, Z. J. and H. Gao. 2009. A unifying lifting collocation penalty formulation including the Discontinuous Galerkin, Spectral Volume/ Difference methods for conservation laws on mixed grids. *J. Comput. Phys.* 228: 8161-8186
- [12] Bassi, F. and S. Rebay. 1997. A high-order accurate discontinuous finite element method for the numerical solution of the compressible Navier-Stokes equations. *J. Comput. Phys.* 131: 267-279
- [13] Huynh, H. T. 2009. A reconstruction approach to high-order schemes including Discontinuous Galerkin for diffusion. *AIAA paper* 2009-403
- [14] Gottlieb, S., C. W. Shu and E. Tadmor. 2001. Strong stability-preserving high-order time discretization methods. *SIAM Rev.* 43: 89-112
- [15] Menter, F. R., R. B. Langtry, S. R. Likki, Y. B. Suzen, P. G. Huang and S. Völker. 2006. A correlation-based transition model using local variables – Part I: model formulation. *J. Turbomach.* 128: 413-422.
- [16] Wang L. and S. Fu. 2011. Development of an intermittency equation for the modelling of the supersonic/hypersonic boundary layer flow transition. *Flow, Turbul. and Combust.* 87: 165-187